THE JOURNAL OF PHYSICAL CHEMISTRY B

ARTICLE

pubs.acs.org/JPCB

Prediction of the PC-SAFT Associating Parameters by Molecular Simulation

Nicolas Ferrando,*[,†] Jean-Charles de Hemptinne,[†,§] Pascal Mougin,[†,§] and Jean-Philippe Passarello[‡,§]

[†]IFP Energies nouvelles, 1 et 4 Avenue de Bois-Préau, 92852 Rueil-Malmaison Cedex, France

[‡]LSPM, 99, av. Jean-Baptiste Clément, 93430 Villetaneuse, France

ABSTRACT: In this work, we propose a new methodology to determine association scheme and association parameters (energy and volume) of a SAFT-type EoS for hydrogen-bonding molecules. This paper focuses on 1-alkanol molecules, but the new methodology can also be applied for any other associating system. The idea is to use molecular simulation technique to determine independently monomer and free hydrogen fractions from which the association scheme can be deduced. The 3B scheme thus appeared to be the most appropriate for 1-alkanols. Once the association scheme is defined, the association strength can be back-calculated from molecular simulation results and used as an independent property for the equation of state parameters regression, in addition of the classical phase properties such as vapor pressure and liquid molar volume. A new set of parameters for 1-alkanol for the PPC-SAFT equation of state has been proposed following this methodology. Results are found in good agreement with experimental data for both phase properties and free hydrogen-bonding sites. Hence, this new methodology makes it possible to optimize parameters allowing an accurate reproduction of pure compounds data and yielding physically significant values for associating energy and associating volume.

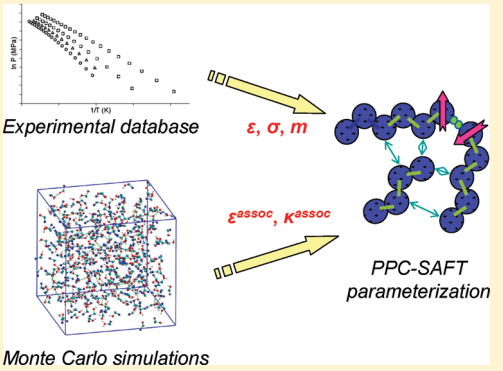

1. INTRODUCTION

When specific chemical forces act between molecules, there is the possibility of complex formation. This phenomenon is called association or self-association when it occurs between like molecules, and solvation or cross-association when the molecules are different.

The explicit introduction of the association phenomenon in equations of state has been attempted by many authors. The various approaches have been very well summarized in the recent book of Kontogeorgis and Folas.[1] Three types of approaches can be identified. One of the first attempts was published by Heidemann and Prausnitz in 1976.[2] They consider the possibility of molecules to form multimers according to chemical equilibria. Using a cubic equation of state (EoS) and reasonable assumptions, they obtain a closed-form expression for the EoS, with one additional parameter, which is the chemical equilibrium constant. This has led to the development of several new equations of state for hydrogen bonding systems, PACT[3,4] and APACT being the most well-known. Anderko[5] has proposed an alternative approach where a specific term was added to the equation of state, which essentially represents the ratio of total mole number to apparent mole number. The chemical equilibrium constant is again used as an additional parameter. Campbell et al.[6] describes in some more details the closed-form expression that results when one or two sites exist on the associating species (i.e., only linear chains can be formed). Today, the most often used approach for associating compounds is that based on the Wertheim first-order thermodynamic perturbation theory[7,8] demonstrated to be correct by Jackson, Chapman, Gubbins, and Radosz[9−11] and demonstrated for real systems and hence reduced to engineering practice by Huang and Radosz.[12] This theory considers the association sites explicitly: instead of considering molecular equilibrium, it is now possible to consider equilibria between sites and therefore differentiate each of these reacting sites on the molecules. The additional parameter, the association strength Δ^{assoc}, is a site−site chemical equilibrium constant. It is the basis for the SAFT equations of state,[1,13,14] but also CPA[15] and GCA.[16]

Economou and Donohue[17] nicely reviewed these different association theories, also including that based on the lattice theory of Sanchez−Lacombe.[18] They conclude that although through different routes, the final results of the various theories have essentially the same mathematical form.

The difficulty of finding adequate parameters to SAFT-type equations of state has been illustrated by Clarke for water:[19] the problem is strongly degenerate because the dispersive and association contribution really have the same macroscopic effect ("attraction"). This leads to a difficulty in correctly identifying physically based parameters for such equations of state. Several options have been used for solving this problem. Mourah et al.,[20] for example, use some binary mixture data to add additional constraints. Wolbach and Sandler[21] propose to use molecular orbital calculation for determining the hydrogen-bonding parameters.

Received: September 27, 2011
Revised: November 21, 2011
Published: November 29, 2011

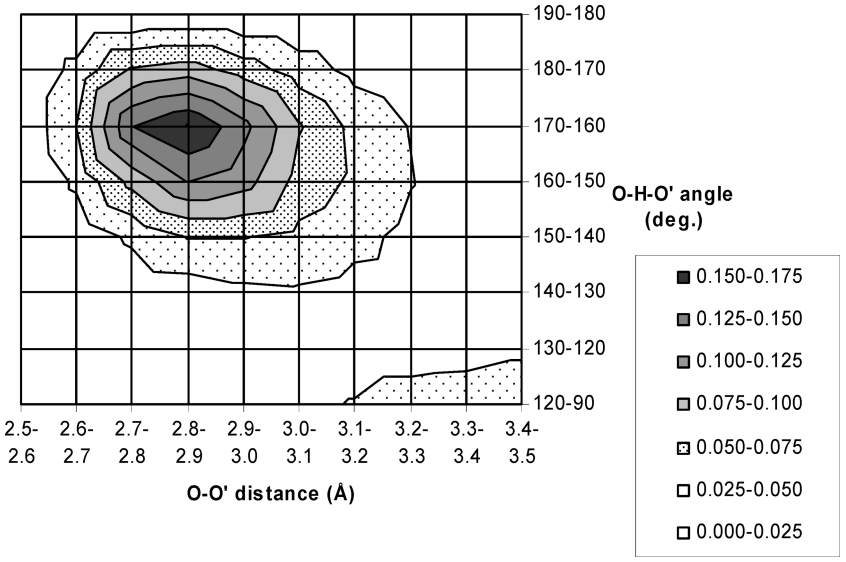

Figure 1. Distribution of oxygen−oxygen contacts in methanol at 300 K as a function of the O−O′ distance and the O−H--O′ angle. Results obtained from Monte Carlo simulation using the AUA4 force field.

Other authors use the number of monomers or the number of free hydrogen-bonding sites as a criterion to evaluate what hydrogen-bonding scheme is preferable in the SAFT model.[22] Lately, this additional property has been used as an additional, independent piece of information for parametrizing the EoS.[23]

In this work, we propose a new methodology, based on structural properties predicted by Monte Carlo molecular simulation, whose aim is to determine:

(1) the association scheme of a given molecule, that is, the maximum number of independent sites in a molecule able to form a hydrogen bond,

(2) the corresponding energy and volume association parameters for the PPC-SAFT equation of state (Nguyen-Huynh[24]) that is based on the PC-SAFT proposed by Gross and Sadowski,[25,26] combined with a polar term as proposed by Gubbins and Twu[27] and extended by Jog and Chapman.[28]

Note that the methodology is not restricted to this specific equation of state but can be theoretically applied to any equation including an associative term based on the Wertheim theory (e.g., SAFT-0 (Chapman et al., 1990[11]), SAFT-VR (Gil-Villegas et al., 1997[29]), soft-SAFT (Blas and Vega, 1998[30]), CPA (Kontogeorgis et al., 1996[15]), ...). The idea is to determine the association strength Δ^{assoc} from the structural properties computed during the molecular simulations, and to calculate the association parameters ε^{assoc} and κ^{assoc} from this association strength for a given set of segment (ε and σ) and chain (m) parameters. This new methodology can be easily implemented in parameters regression codes: when segment and chain parameters are adjusted to reproduce VLE properties (classically, saturated liquid densities, vapor pressures, vaporization enthalpies, ...), the corresponding association parameters are calculated from molecular simulation data at each iteration of the fitting procedure. In this way, the goal of this methodology is to reduce the number of parameters to be adjusted, and to give a physical coherence between the parameter sets of the dispersive−repulsive and the associative parts of the equation of state. As a consequence, it should make the equation of state able to predict simultaneously VLE properties and structure properties such as monomer fractions. To illustrate this new approach, we specifically focus in this work on 1-alkanols, but any other kind of associative molecule could be studied in a similar manner.

In the first part of this paper we describe how molecular simulation can be used with an adapted force field to generate structural data such as monomer fractions or free hydrogen fractions in a liquid bulk. The Monte Carlo technique is used in this work, but similar information could also be generated using the molecular dynamic technique. In a second part, the methodology developed to determine the association scheme and the association parameters from the molecular simulation results is described. The third part illustrates this approach with the adjustment of new PPC-SAFT parameters of 1-alkanols. Finally, the fourth section gives our conclusions.

2. PREDICTION OF STRUCTURAL PROPERTIES BY MONTE CARLO SIMULATIONS

2.1. Simulation Details. The Monte Carlo simulations are carried out in the *NVT* Gibbs ensemble (Panagiotopoulos[31,32]). A total number of 400 molecules was used for each system investigated, and the simulation runs lasted for 60 million steps (including an equilibration run of 30 million steps), one step corresponding to a single Monte Carlo move. For Lennard-Jones interactions, a spherical cutoff equal to half the simulation box was used, and classical tail correction was employed.[33] For long-range electrostatic energy, the Ewald sum technique was used, with a number of reciprocal vectors k ranging from −7 to +7 in all three directions and a Gaussian width α equal to 2 in reduced units. The different Monte Carlo moves and their attempt probabilities that were used during the simulations are translation (15%), rigid rotation (15%), configurational-bias regrowth[34] (20%), transfer with insertion bias[35] (49.5%), and volume change (0.5%). The amplitude of translations, rotations, and volume changes was adjusted during the simulation to achieve an acceptance ratio of 40% for these moves. The AUA4 force field is used to model the alcohol molecules involved in this work.[36] This choice is motivated by the ability of this force field to accurately predict both thermodynamic saturated properties (density, vapor pressure, vaporization enthalpies) and liquid phase structure (radial distribution functions, hydrogen bond networks).

Table 1. Liquid Phase Properties from Monte Carlo Simulations[a]

	Monte Carlo simulations results					Monte Carlo simulations results			
temp (K)	density (mol/m^3)	monomer fraction (X^m)	free hydrogen fraction (X^H)	association strength Δ (eq 10) (m^3 mol^{-1})	temp (K)	density (mol/m^3)	monomer fraction (X^m)	free hydrogen fraction (X^H)	association strength Δ (eq 10) (m^3 mol^{-1})
				Methanol					
275	25465	0.006_1	0.029_6	0.001794	425	20272	0.091_4	0.237_{10}	0.000150
300	24782	0.014_2	0.050_7	0.000846	450	18886	0.127_5	0.291_{11}	0.000113
325	23958	0.023_2	0.077_7	0.000537	475	17553	0.173_7	0.354_{14}	0.000086
375	22325	0.048_3	0.144_9	0.000271					
				Ethanol					
275	17749	0.007_1	0.029_6	0.002296	425	14341	0.127_6	0.292_{14}	0.000146
300	17274	0.014_2	0.055_9	0.001208	450	13540	0.171_7	0.356_{14}	0.000108
325	16811	0.023_2	0.083_8	0.000693	475	12507	0.232_6	0.434_{12}	0.000080
375	15626	0.062_3	0.172_9	0.000279					
				1-Propanol					
300	13361	0.016_2	0.060_9	0.001279	450	10627	0.219_5	0.420_{10}	0.000101
350	12609	0.051_4	0.149_{11}	0.000422	500	8987	0.370_8	0.575_{13}	0.000058
400	11677	0.117_6	0.279_{13}	0.000185					
				1-Butanol					
300	10978	0.015_2	0.061_9	0.001605	450	8868	0.242_5	0.439_9	0.000103
350	10405	0.056_5	0.159_{15}	0.000453	500	7820	0.381_{10}	0.589_{16}	0.000062
400	9725	0.131_5	0.292_{12}	0.000199					
				1-Pentanol					
300	9323	0.015_1	0.057_4	0.001870	450	7674	0.264_5	0.464_{10}	0.000108
350	8849	0.060_4	0.165_{11}	0.000496	500	6902	0.402_8	0.603_{12}	0.000065
400	8309	0.142_6	0.308_{13}	0.000209					
				1-Hexanol					
300	8105	0.025_4	0.081_{11}	0.001301	450	6729	0.276_8	0.476_{13}	0.000115
350	7708	0.066_4	0.176_{12}	0.000514	500	6102	0.420_7	0.619_{10}	0.000067
400	7242	0.156_6	0.324_{13}	0.000216					
				1-Heptanol					
300	7164	0.026_4	0.082_{13}	0.001437	450	5995	0.301_6	0.500_{10}	0.000113
350	6843	0.067_3	0.172_9	0.000573	500	5482	0.441_6	0.637_8	0.000069
400	6448	0.161_6	0.329_{11}	0.000233					
				1-Octanol					
300	6431	0.020_4	0.068_{12}	0.001684	450	5410	0.310_9	0.509_{15}	0.000120
320	6312	0.038_8	0.117_{26}	0.001095	500	4994	0.460_{11}	0.652_{15}	0.000070
340	6212	0.060_3	0.157_9	0.000704	550	4504	0.586_8	0.751_{10}	0.000047
400	5810	0.169_4	0.342_9	0.000244					

[a] The subscripts give the statistical uncertainty on the last decimal (for example: 0.013_2 means 0.013 ± 0.002).

Structural properties of the liquid phase are studied using equilibrated configurations generated during the simulations. A geometric criterion is used to determine whether a hydrogen bond exists or not: by analyzing the distribution of the oxygen−oxygen contacts as a function of the O−O′ distance and the O−H--O′ angles (Figure 1), the first solvation shell related to the hydrogen bond formation corresponds to O−O′ distances ranging from 2.5 and 3.5 Å, and O−H--O′ angles ranging from 120 to 180°. From this hydrogen bond definition, some specific structural properties can be calculated. One of them is the *monomer fraction* X^m defined as the ratio between the number of alcohol molecules not involved in a hydrogen bond and the total number of alcohol molecules in the bulk. Another important structural property is the *free hydrogen fraction* X^H, defined as the ratio between the number of hydroxyl hydrogen atoms not involved in a hydrogen bond and the total number of hydroxyl hydrogen atoms. It is worth noticing that these two structural properties are determined independently from each other, only by numbering molecules and atoms obeying to the hydrogen bonds criteria defined above in the equilibrated configurations.

2.2. Validation. The 1-alkanol series (from methanol to 1-octanol) has been simulated for reduced temperatures ranging from 0.52 to 0.92. Table 1 reports both predicted monomer and free hydrogen fractions, and Figure 2 compares simulation results and a

dx.doi.org/10.1021/jp209313a |J. Phys. Chem. B 2012, 116, 367–377

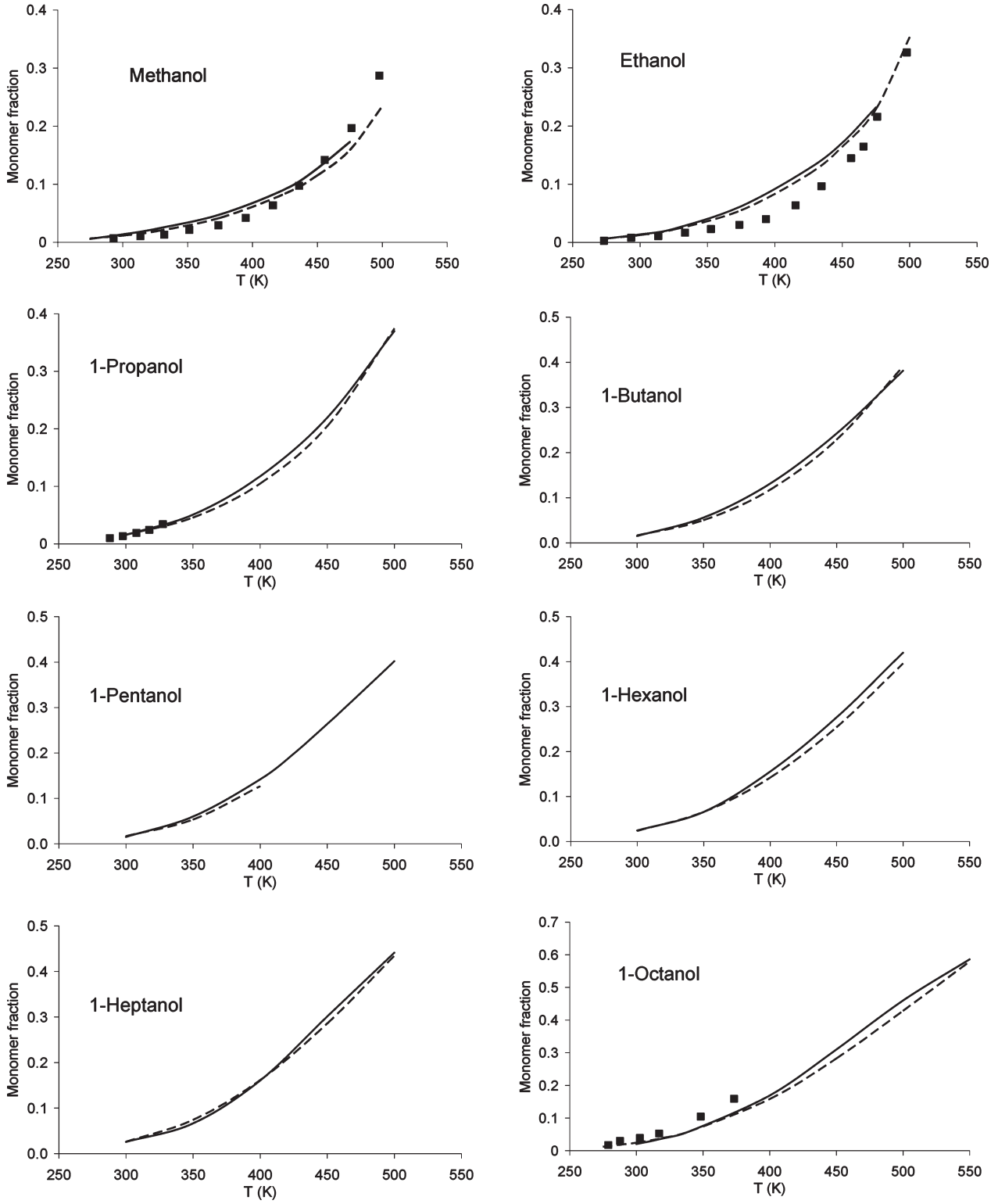

Figure 2. Monomer fraction in pure 1-alkanols. Filled symbols stand for experimental data reported by Kontogeorgis et al.[23] Solid lines are a fit of the Monte Carlo simulation results. Dashed lines stand for the PPC-SAFT results using the parameters proposed in this work.

compilation of experimental data reported by Kontogeorgis et al.[23] when available (methanol, ethanol, 1-propanol, and 1-octanol).

For methanol and 1-propanol, a good agreement between simulation and experimental data is reached. It is important to recall that the geometric criteria previously described to define the hydrogen bond have been selected independently of the experimental data, exhibiting thus the predictivity of this approach. Predictions slightly underestimate the monomer fraction of 1-octanol, but it is worth noticing that a similar behavior has already been observed using associative equations of state

dx.doi.org/10.1021/jp209313a |*J. Phys. Chem. B* 2012, 116, 367–377

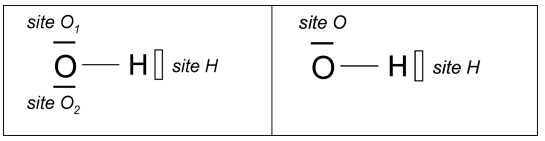

Figure 3. 3B (left) and 2B (right) association schemes in alcohol.

(Tsivintzelis et al.,[37] Kontogeorgis et al.[23]). Although both experimental data and Monte Carlo simulation results suggest an increase of the monomer fraction with the alkyl chain length for a given temperature, experimental monomer fractions of ethanol are surprisingly very close to those of methanol. Such a trend is questionable, making the comparison between our simulation results and experiments for this compound not obvious.

3. DETERMINATION OF THE ASSOCIATION SCHEME AND PARAMETERS FROM MOLECULAR SIMULATION DATA

3.1. Determination of the Association Scheme. Using the Wertheim theory of association, it is important to define how the molecules interact with each other: the number of association sites and their type (electron donor or electron acceptor). According to the classification of Huang and Radosz,[12] two possibilities should be considered for alcohols. In addition to the electron acceptor capacity of the hydrogen atom, one may consider either the two free electron pairs of the oxygen atom independently as two electron donors, making it a three-site molecule (generally known as 3B). On the other hand, one considers that steric hindrance makes that only one of the two free electron pairs is really active, making it a two-site molecule (known as 2B). The two options are illustrated in Figure 3. Note that a 2C assocation scheme involving two electron donor sites and one bipolar site has also been recently proposed.[38] No clear agreement exists among the authors who have discussed the use of an association EoS with alcohols concerning this choice.

Von Solms et al.[22,39] proposes a direct comparison with the monomer fractions as obtained from experiment. In this paper, we extend their arguments by using information obtained from molecular simulation. In this section we present two approaches whose aim is to give information about the association scheme from Monte Carlo simulation results.

3.1.1. From the Distribution of Hydrogen Bonds Number per Molecule. It is well-known from experimental (e.g., Harvey,[40] Wertz et al.,[41] Narten et al.,[42] Yamaguchi et al.,[43] Lin et al.[44]) and molecular simulation (Jorgensen,[45−47] Chen et al.,[48] Ferrando et al.,[36] Schnabel et al.[49]) studies that the *average* number of hydrogen bonds per alcohol molecule is close to 2 at room temperature. However, because the association scheme is related to the *maximal* number of hydrogen bonds per molecule, it is necessary to determine if configurations with more than 2 hydrogen bonds per molecule can be found with a significant weight in the system. From our Monte Carlo simulation results, the distribution of hydrogen bonds number per molecule in methanol at 300 K is plotted on Figure 4. This figure exhibits that more than 85% of molecules are involved at maximum in two hydrogen bonds. However, the part of molecules involved in three hydrogen bonds, that is, with three association sites, cannot be reasonably neglected (about 15%). Note that such results are consistent with similar simulations performed using specific force field for methanol.[46,49] Such a result shows that the maximal number

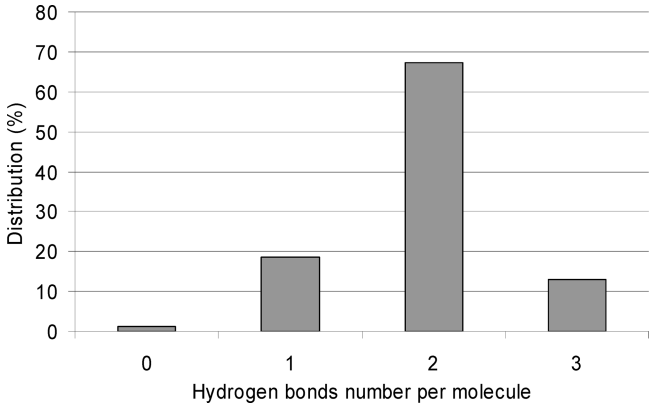

Figure 4. Distribution of the hydrogen bonds number per molecule of methanol at 300 K.

of sites to be considered is preferentially 3. This is a first indication, rather qualitative, to guide the choice of the association scheme.

3.1.2. From Monomer and Free Hydrogen Fractions. Another indication can be found in a more quantitative manner by establishing a relationship between the monomer fraction and the free hydrogen fraction determined from the Monte Carlo simulations. Let us denote O_1, O_2, and H the three association sites in a 3B scheme, and O and H the two association sites in a 2B scheme (Figure 3).

From a general point of view, the probability that a molecule is not hydrogen-bonded to another is equal to the probability that all the association sites of this molecule are free (that is, not involved in a hydrogen bond):

$$X^{\mathrm{m}} = \prod_{i=1}^{N} X^{i} \tag{1}$$

where X^i denotes the site of type i and N the total number of type of sites in the molecule. In the cases of a 3B and 2B association scheme, eq 1 becomes

$$X^{\mathrm{m}} = X^{\mathrm{O_1}} X^{\mathrm{O_2}} X^{\mathrm{H}} \qquad \text{in a 3B scheme} \tag{2}$$

$$X^{\mathrm{m}} = X^{\mathrm{O}} X^{\mathrm{H}} \qquad \text{in a 2B scheme} \tag{3}$$

Von Solms et al.[22] established some relationships between free site fractions in both schemes. In a 3B scheme, the two sites O_1 and O_2 have an equal probability of bonding, leading to the relation

$$X^{\mathrm{O_1}} = X^{\mathrm{O_2}} \tag{4}$$

Second, because for every H site involved in a hydrogen bond, an O site in the system is also bonded, a material balance over the number of sites gives

$$1 - X^{\mathrm{H}} = 2(1 - X^{\mathrm{O_1}}) \qquad \text{in a 3B scheme} \tag{5}$$

$$1 - X^{\mathrm{H}} = 1 - X^{\mathrm{O}} \qquad \text{in a 2B scheme} \tag{6}$$

From these relationships, eqs 2 and 3 can be rewritten in term of free hydrogen fraction:

$$X^{\mathrm{m}} = \frac{(X^{\mathrm{H}} + 1)^2 (X^{\mathrm{H}})}{4} \qquad \text{in a 3B scheme} \tag{7}$$

$$X^{\mathrm{m}} = (X^{\mathrm{H}})^2 \qquad \text{in a 2B scheme} \tag{8}$$

dx.doi.org/10.1021/jp209313a |J. Phys. Chem. B 2012, 116, 367–377

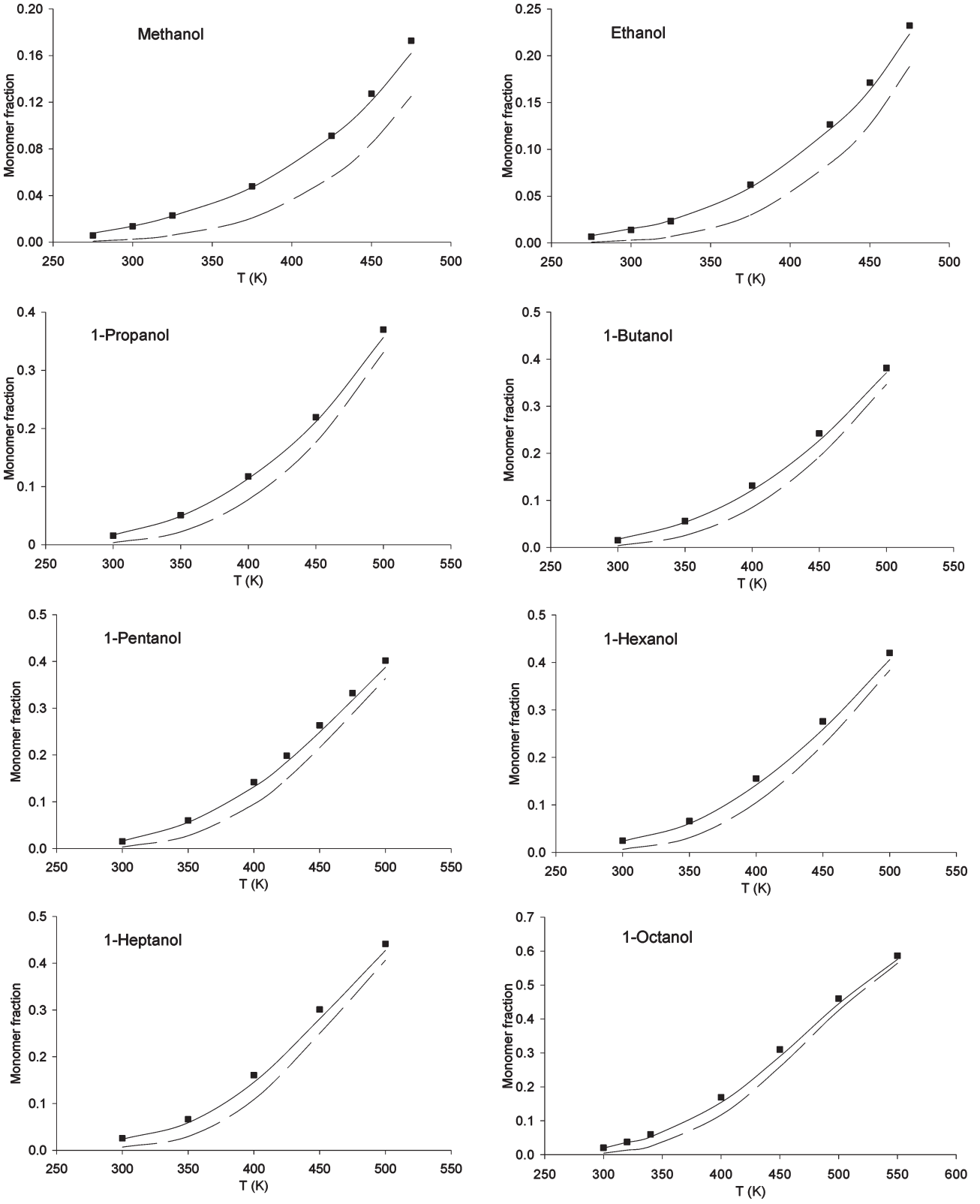

Figure 5. Monomer fraction in 1-alkanols from Monte Carlo simulations (symbols), eq 7 (3B association scheme, solid lines), and 8 (2B association scheme, dashed lines).

For each free hydrogen fractions resulting from Monte Carlo simulations and presented in Table 1, the monomer fraction is calculated for 1-alkanols using either eq 7 or eq 8, and results are compared in Figure 5 to the Monte Carlo monomer fractions.

dx.doi.org/10.1021/jp209313a |*J. Phys. Chem. B* 2012, 116, 367–377

It clearly appears that for all the studied alcohols, the assumption of a 3B association scheme is in better accordance with the Monte Carlo simulation results.

3.2. Determination of the Association Energy and Volume Parameters. According to Huang and Radosz[12] for a 3B association scheme, the free site fraction is related to the association strength Δ by the relationship:

$$X^{O_1} = X^{O_2} = \frac{1}{2}(X^H + 1) = \frac{-(1-\rho\Delta) + \sqrt{(1+\rho\Delta)^2 + 4\rho\Delta}}{4\rho\Delta} \quad (9)$$

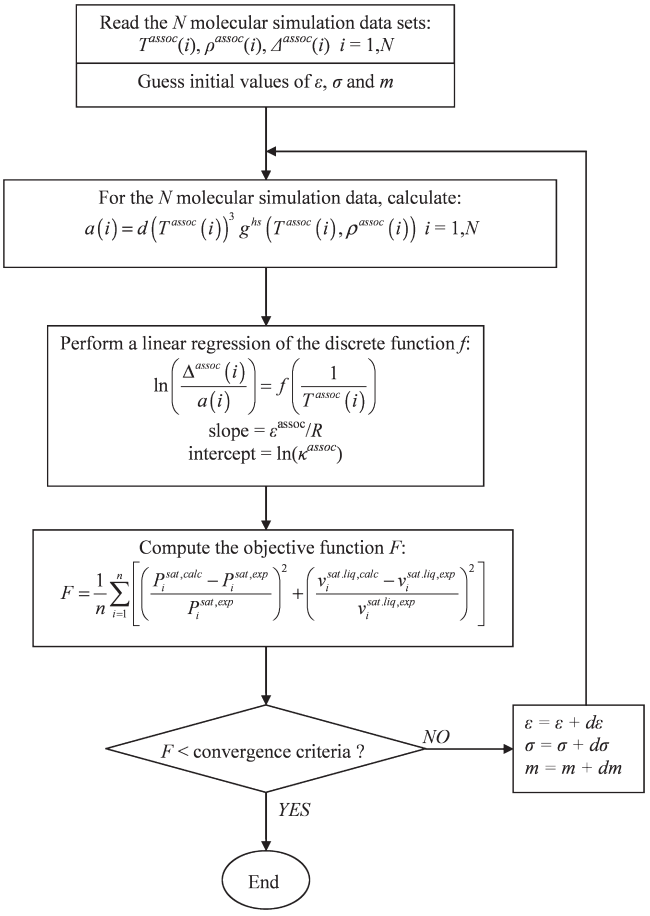

Figure 6. Parameter fitting algorithm.

where ρ is the molar density of the system. Note that with this formalism, the association strength has the dimension of a molar volume. Using eq 7, the monomer fraction is consequently related to the association strength by the relation[23]

$$X^m = \frac{(\rho\Delta)^2 - 4\rho\Delta - 1 + (\rho\Delta + 1)\sqrt{(\rho\Delta + 1)^2 + 4\rho\Delta}}{8(\rho\Delta)^3} \quad (10)$$

From molar densities and monomer fractions determined by the Monte Carlo simulations, the association strength Δ is calculated from eq 10 for each compound and temperature. Results are reported in Table 1. Furthermore, in the SAFT equation of state formalism, the association strength between a site O_1 (or O_2) in a molecule i and a site H in a molecule j is given by

$$\Delta^{O_{1,i}H_j} = d_{ij}^3 g^{hs} \kappa^{O_{1,i}H_j}\left[\exp\left(\frac{\varepsilon^{O_{1,i}H_j}}{RT}\right) - 1\right] \quad (11)$$

where d_{ij} is the hard sphere diameter, g^{hs} is the hard sphere radial distribution function, $\kappa^{O_{1,i}H_j}$ is the association volume parameter, $\varepsilon^{O_{1,i}H_j}$ the association energy parameter, R is the ideal gas constant, and T is the temperature. We further assume that the term $\exp[\varepsilon^{O_{1,i}H_j}/RT]$ is much greater than unity:

$$\exp\left(\frac{\varepsilon^{O_{1,i}H_j}}{RT}\right) \gg 1 \quad (12)$$

This assumption will be checked a posteriori once $\varepsilon^{O_{1,i}H_j}$ determined. Considering pure compound systems, eq 11 can thus be rewritten

$$\ln\left(\frac{\Delta^{O_1H}}{a(T)}\right) = \frac{\varepsilon^{O_1H}}{RT} + \ln(\kappa^{O_1H}) \quad (13)$$

with

$$a(T) = d(T)^3 g^{hs}(T) \quad (14)$$

In the PC-SAFT version, the hard sphere diameter is related to the segment parameter σ with:

$$d(T) = \sigma\left[1 - 0.12\exp\left(-\frac{3\varepsilon}{RT}\right)\right] \quad (15)$$

where ε is the well depth of the dispersive−repulsive potential. The hard sphere radial distribution function proposed by

Table 2. Optimized PPC-SAFT Parameters for 1-Alkanols

	adjusted parameters			resulting parameters (from molecular simulation)		fixed parameters	
	ε/R (K)	σ (Å)	m	ε^{assoc}/R (K)	κ^{assoc}	μ (D)	$x_p m$
methanol	176.30	2.6476	2.9232	1486.29	0.1701	1.70	0.5
ethanol	191.32	2.9384	3.0790	1771.89	0.0602	1.70	0.5
1-propanol	199.21	3.0456	3.5664	1846.57	0.0424	1.70	0.5
1-butanol	214.09	3.2389	3.7099	1979.07	0.0255	1.70	0.5
1-pentanol	239.65	3.5375	3.4355	2078.14	0.0150	1.70	0.5
1-hexanol	228.39	3.4056	4.3273	1829.61	0.0320	1.70	0.5
1-heptanol	233.02	3.5018	4.6664	1900.37	0.0242	1.70	0.5
1-octanol	242.49	3.6090	4.7118	1957.72	0.0206	1.70	0.5

dx.doi.org/10.1021/jp209313a |J. Phys. Chem. B 2012, 116, 367–377

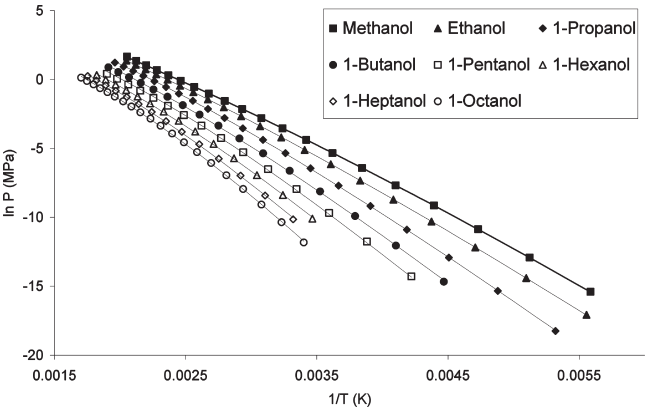

Figure 7. Vapor pressures of 1-alkanols. Symbols: experimental data (from DIPPR database). Lines: PPC-SAFT results.

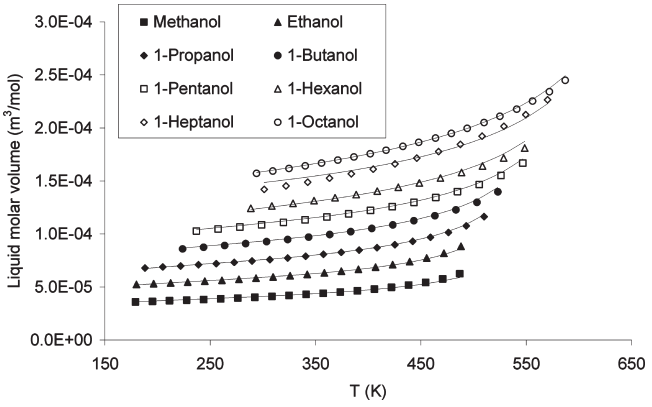

Figure 8. Saturated liquid molar volume of 1-alkanols. Symbols: experimental data (from DIPPR database). Lines: PC-SAFT results.

Boublik[50] is used. For pure compounds its expression is reduced to

$$g^{\mathrm{hs}}(T) = \frac{2-\zeta_3}{2(1-\zeta_3)^3} \tag{16}$$

with

$$\zeta_3(T) = \frac{\pi}{6} N_a m d^3 \rho(T) \tag{17}$$

where N_a is the Avogadro number and m is the chain parameter.

For each compounds and according to eq 13, plotting $\ln[\Delta^{O_1H}/a(T)]$ as a function of $1/T$ allows us to determine the energy (slope of the curve) and volume (intercept of the curve) association parameters.

4. PARAMETRIZATION OF THE PPC-SAFT EQUATION OF STATE USING MOLECULAR SIMULATION DATA

In this section, we propose a parametrization of the Polar PC-SAFT EoS (PPC-SAFT) for 1-alkanols in using the previously described methodology to calculate the association parameters $\varepsilon^{\mathrm{assoc}}$ and κ^{assoc}. The equation is a combination of the PC-SAFT EoS by Gross and Sadowski,[25,26] that includes a polar contribution as discussed by Nguyen-Huynh et al.[24] For each pure compound, the adjustable parameters are the segment parameters ε and σ and the chain parameter m. For the 1-alkanols

Table 3. Vapour Pressures and Saturated Liquid Volumes Deviations between Experimental (from DIPPR Data Base) and Calculated Values[a]

	T range (K)	AAD P^{sat} (%)	AAD $v^{\mathrm{sat\ liq}}$ (%)
methanol	179−487	1.3	1.3
ethanol	180−488	1.0	0.6
1-propanol	188−510	2.8	0.6
1-butanol	224−523	5.5	1.0
1-pentanol	237−547	5.0	1.1
1-hexanol	289−549	5.1	0.9
1-heptanol	301−570	5.3	0.8
1-octanol	294−587	4.5	0.4

[a] AAD (%) = $\{[\mathrm{abs}(X^{\mathrm{calc}} - X^{\mathrm{exp}}]/X^{\mathrm{exp}}\} \cdot 100$.

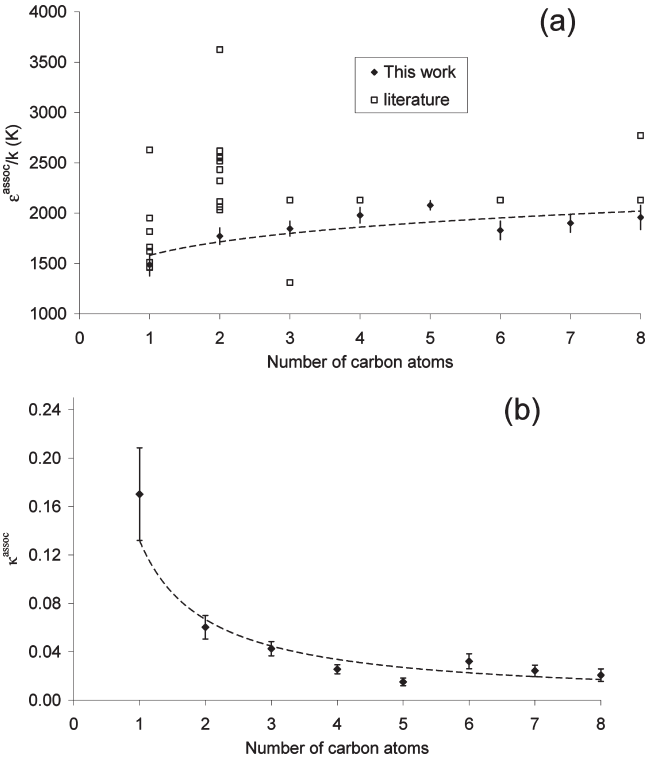

Figure 9. Association energy (a) and association volume (b) vs length of the alkyl chain in 1-alkanols. Filled symbols: this work. Open symbol: compilation of experimental data reported in literature (Table 4). Lines are a guide for the eyes.

investigated, the dipole moment μ is taken equal to 1.70 D and the dipole fraction $x_p m$ is equal to 0.5 according to the recommendations of Nguyen-Huynh et al.[24] The parameters regression algorithm is described on Figure 6. It is based on the use of eq 13, which allows determining both values of ε^{O_1H} and κ^{O_1H} at once. Iterations are needed because the value of $a(T)$ itself depends on the values of the nonassociative parameters ε, σ, and m.

The experimental VLE data used in the regression are vapor pressures and liquid saturated volumes. They all originate from the DIPPR database. The fitted PPC-SAFT parameters as well as the resulting association parameters are given in Table 2. Note that the obtained association energy parameters are consistent with the assumption described by eq 12. Figures 7 and 8 show a comparison between experimental and calculated data with these

dx.doi.org/10.1021/jp209313a | J. Phys. Chem. B 2012, 116, 367–377

Table 4. Literature Values for the Enthalpy of Association

component	method	association enthalpy kJ/mol	association enthalpy K	ref
methanol−methanol	"second virial coefficients"	13.82	1662	51
	"flow calorimeter"	13.48	1621	52
	infrared photodissociation	12.14	1460	53
	absorption infrared radiation	12.56	1511	54
	methanol in hexadecane	12.2	1465	55
	calorimetry	15.1	1816	56
	heat of vaporization comparison with alkane homomorph	21.9	2629	57
	molecular orbital calculations	16.2	1951	58
	chromatography			
ethanol−ethanol	calorimetry	16.9	2033	56
	spectroscopy	20.9	2517	59
	infrared spectroscopy	21.31	2563	60
	Fourier transform	17.6	2114	61
	infrared (FTIR) spectra	17.6	2114	
	infrared spectroscopy	19.30	2321	62
	infrared spectroscopy	20.2	2432	63
	infrared spectroscopy	21.77	2618	64
	NMR	30.1	3625	65
	heat of vaporization comparison with alkane homomorph	21.2	2549	57
	molecular orbital calculations	17.2	2063	58
1-propanol−1-propanol	spectroscopy	10.9	1310	59
	calorimetry	17.7	2129	56
2-propanol−2-propanol	calorimetry	17.3	2081	56
1-butanol−1-butanol	calorimetry	17.7	2129	56
1-hexanol−1-hexanol	calorimetry	17.7	2129	56
1-octanol−1-octanol	calorimetry	17.7	2129	56
	spectrophotometric	23.03	2770	66
	spectroscopy	22.4		67

optimized parameters for vapor pressure and saturated liquid molar volume, respectively, and Table 3 gives the average deviations obtained on vapor pressure and liquid volume predictions.

A trend is observed when looking at the association parameter as a function of the chain length (Figure 9). The association energy increases with alcohol chain length and the association volume decreases. Using regular parameter regression, this phenomenon cannot be observed because both parameters are degenerated: increasing the energy of association or decreasing the volume of association has the same global effect on the association strength. Using the proposed approach, it is now possible to distinguish the two values. The energy of association is to be compared with the enthalpy of hydrogen bonding, and the volume is related to the entropy of association. Data for these properties exist but are very scattered, as witnessed by the values shown in Table 4, also reported in Figure 9. The trend can be explained by observing that the longer the chain length, the larger the steric hindrance between species resulting in a decreasing association volume.

To validate the parameter values, we discuss them in comparison with other investigations that use the same PPC-SAFT model. Methanol was treated independently of the other alcohols by Mourah et al.,[20] because the phase behavior of this small alcohol is quite different from that of the other alcohols (it forms a liquid−liquid phase split with *n*-alkanes). Testing both 2B and 3B schemes on both LLE and VLE of methanol + *n*-alkane mixtures, they concluded that the 2B scheme was better adapted. Their parameters are quite similar to ours, except larger values for the association energy (2069 K for 2B vs 1486 K in this work) and the association volume (0.237 for 2B vs 0.17 in this work). Regarding the longer chain alcohols (from ethanol onward), the deviations obtained by Nguyen-Huynh et al.[24] using the same EoS and the same 3B association scheme are generally larger because they use a group contribution scheme, thus reducing the number of adjustable parameters. Their association parameters are unique, equal to $\varepsilon^{O_1H} = 2082.06$ K (a bit larger than ours) and $\kappa^{O_1H} = 0.0238$ (similar to ours).

Finally, as we assumed a 3B scheme for 1-alkanol, the monomer fractions for each pure system are calculated from the site nonbonded fraction extracted from the PPC-SAFT calculations with eq 2. For each compound, these monomer fractions are plotted in Figure 2. As association parameters are determined from structural properties generated by Monte Carlo simulations, it is not surprising to find that such quantities are in good agreement with experimental data. It is, however, worth noticing that obtaining accurate results on both VLE properties and liquid phase structure with an equation of state is not obvious, and this methodology gives an opportunity to reach this goal with only three adjustable parameters.

5. CONCLUSION

This paper proposes an alternative approach for determining the parameters of a SAFT-type EoS (or any equation of state including an associative term based on the Wertheim theory) for hydrogen-bonding molecules. Using Monte Carlo simulation, it is possible to determine independently the monomer fraction (X^m) and the nonbonded sites fraction (X^H, for example, when considering the proton-donor sites) of a hydrogen-bonding molecule. Using this feature, and the relationships that can be constructed for relating these two quantities, it has been shown that for 1-alcohols, a 3B association scheme is the best one.

Once the association scheme is determined, it is possible to use the nonbonded sites fraction to back-calculate the association strength, which can now be used as an independent piece of information. The parameters are then regressed using this in addition to the vapor pressure and the liquid molar volume.

The parameters that are thus found are able to reproduce correctly the pure component data, and yield physically significant values for the association energy and association volume.

AUTHOR INFORMATION

Corresponding Author

*Tel: +33 147526624. Fax: +33 147527025. E-mail: nicolas.ferrando@ifpen.fr.

Notes

§E-mail: J.-C.d.H., j-charles.de-hemptinne@ifpen.fr; P.M., pascal.mougin@ifpen.fr; J.-P.P., jean-philippe.passarello@lspm.cnrs.fr.

REFERENCES

(1) Kontogeorgis, G. M.; Folas, G. K. *Thermodynamic Models for Industrial Applications: From Classical and Advanced Mixing Rules to Association Theories*; Wiley: New York, 2010.
(2) Heidemann, R. A.; Prausnitz, J. M. *Proc. Natl. Acad. Sci. U. S. A.* **1976**, *73* (6), 1773–1776.
(3) Ikonomou, G. D.; Donohue, M. D. *AIChE J.* **1986**, *32* (10), 1716–1725.
(4) Ikonomou, G. D.; Donohue, M. D. *Fluid Phase Equilib.* **1988**, *39*, 129–159.
(5) Anderko, A. *Fluid Phase Equilib.* **1992**, *75*, 89–103.
(6) Campbell, S. W.; Economou, I. G.; Donohue, M. D. *AIChE J.* **1992**, *38* (4), 611–614.
(7) Wertheim, M. S. *J. Stat. Phys.* **1984**, *35*, 35–47.
(8) Wertheim, M. S. *J. Stat. Phys.* **1986**, *85*, 2929.
(9) Chapman, W. G.; Jackson, G.; Gubbins, K. E. *Mol. Phys.* **1988**, *65*, 1057–1079.
(10) Jackson, G.; Chapman, W. G.; Gubbins, K. E. *Mol. Phys.* **1988**, *65* (1), 1–31.
(11) Chapman, W. G.; Gubbins, K. E.; Jackson, G.; Radosz, M. *Ind. Eng. Chem. Res.* **1990**, *29*, 1709–1721.
(12) Huang, S. H.; Radosz, M. *Ind. Eng. Chem. Res.* **1990**, *29*, 2284–2294.
(13) Tan, S. P.; Adidharma, H.; Radosz, M. *Ind. Eng. Chem. Res.* **2008**, *47* (21), 8063–8082.
(14) Muller, E. A.; Gubbins, K. E. *Ind. Eng. Chem. Res.* **2001**, *40*, 2193–2211.
(15) Kontogeorgis, G. M.; Voutsas, E. C.; Yakoumis, I. V.; Tassios, D. P. *Ind. Eng. Chem. Res.* **1996**, *35* (11), 4310–4318.
(16) Gros, H. P.; Bottini, S.; Brignole, E. A. *Fluid Phase Equilib.* **1996**, *116* (1−2), 537–544.
(17) Economou, I. G.; Donohue, M. D. *AIChE J.* **1991**, *37* (12), 1875–1894.
(18) Panayiotou, C.; Sanchez, I. C. *J. Phys. Chem.* **1991**, *95* (24), 10090–10097.
(19) Clark, G. N. I.; Haslam, A. J.; Galindo, A.; Jackson, G. *Mol. Phys.* **2006**, *104* (22−24), 3561–3581.
(20) Mourah, M.; NguyenHuynh, D.; Passarello, J. P.; de Hemptinne, J. C.; Tobaly, P. *Fluid Phase Equilib.* **2010**, *298* (1), 154–168.
(21) Wolbach, J. P.; Sandler, S. I. *Ind. Eng. Chem. Res.* **1997**, *36* (10), 4041–4051.
(22) von Solms, N.; Michelsen, M. L.; Passos, C. P.; Derawi, S. O.; Kontogeorgis, G. M. *Ind. Eng. Chem. Res.* **2006**, *45* (15), 5368–5374.
(23) Kontogeorgis, G. M.; Tsivintzelis, I.; von Solms, N.; Grenner, A.; Bøgh, D.; Frost, M.; Knage-Rasmussen, A.; Economou, I. G. *Fluid Phase Equilib.* **2010**, *296* (2), 219–229.
(24) Nguyen-Huynh, D.; Passarello, J. P.; Tobaly, P.; de Hemptinne, J. C. *Fluid Phase Equilib.* **2008**, *264* (1), 62–75.
(25) Gross, J.; Sadowski, G. *Fluid Phase Equilib.* **2000**, *168*, 183–199.
(26) Gross, J.; Sadowski, G. *Ind. Eng. Chem. Res.* **2001**, *40*, 1244–1260.
(27) Gubbins, K. E.; Twu, C. H. *Chem. Eng. Sci.* **1978**, *33*, 863–878.
(28) Jog, P.; Chapman, W. G. *Mol. Phys.* **1999**, *97* (3), 307–319.
(29) Gil-Villegas, A.; Galindo, A.; Whitehead, P. J.; Mills, S. J.; Jackson, G.; Burgess, A. N. *J. Chem. Phys.* **1997**, *106*, 4168–4186.
(30) Blas, F. J.; Vega, L. F. *Ind. Eng. Chem. Res.* **1998**, *37*, 660–674.
(31) Panagiotopoulos, A. Z. *Mol. Phys.* **1987**, *61* (4), 813–826.
(32) Panagiotopoulos, A. Z. *Mol. Sim.* **1992**, *9* (1), 1–23.
(33) Allen, M. P.; Tildesley, D. J. *Computer Simulation of Liquids*; Oxford University Press: Oxford, U.K., 1987.
(34) Frenkel, D.; Smit, B. *Understanding Molecular Simulation: From Algorithms to Applications*; Academic Press: San Diego, 1996.
(35) Mackie, A. D.; Tavitian, B.; Boutin, A.; Fuchs, A. H. *Mol. Simul.* **1997**, *19* (1), 1–15.
(36) Ferrando, N.; Lachet, V.; Teuler, J. M.; Boutin, A. *J. Phys. Chem. B* **2009**, *113* (17), 5985–5995.
(37) Tsivintzelis, I.; Grenner, A.; Economou, I. G.; Kontogeorgis, G. M. *Ind. Eng. Chem. Res.* **2008**, *47* (15), 5651–5659.
(38) de Villiers, A. J.; Schwarz, C. E.; Burger, A. J. *Ind. Eng. Chem. Res.* **2011**, *50*, 8711–8725.
(39) von Solms, N.; Jensen, L.; Kofod, J. L.; Michelsen, M. L.; Kontogeorgis, G. M. *Fluid Phase Equilib.* **2007**, *261* (1−2), 272–280.
(40) Harvey, G. G. *J. Chem. Phys.* **1938**, *6* (3), 111–114.
(41) Wertz, D. L.; Kruh, R. K. *J. Chem. Phys.* **1967**, *47* (2), 388–390.
(42) Narten, A. H.; Sandler, S. I. *J. Chem. Phys.* **1979**, *71* (5), 2069–2073.
(43) Yamaguchi, T.; Hidaka, K.; Soper, A. K. *Mol. Phys.* **1999**, *97* (4), 603–605.
(44) Lin, K.; Zhou, X. G.; Luo, Y.; Liu, S. L. *J. Phys. Chem. B* **2010**, *114* (10), 3567–3573.
(45) Jorgensen, W. L. *J. Phys. Chem.* **1986**, *90* (7), 1276–1284.
(46) Jorgensen, W. L. *J. Am. Chem. Soc.* **1980**, *102* (2), 543–549.
(47) Jorgensen, W. L. *J. Am. Chem. Soc.* **1981**, *103* (2), 345–350.
(48) Chen, B.; Potoff, J. J.; Siepmann, J. I. *J. Phys. Chem. B* **2001**, *105* (15), 3093–3104.
(49) Schnabel, T.; Srivastava, A.; Vrabec, J.; Hasse, H. *J. Phys. Chem. B* **2007**, *111* (33), 9871–9878.
(50) Boublik, T. *J. Chem. Phys.* **1970**, *53*, 471–473.
(51) Kell, G. S.; McLaurin, G. E.; Whalley, E. *J. Chem. Phys.* **1968**, *48*, 3805–3813.
(52) Weltner, W.; Pitzer, K. S. *J. Am. Chem. Soc.* **1951**, *73* (6), 2606–2610.
(53) Hoffbauer, M. A.; Giese, C. F.; Gentry, W. R. *J. Phys. Chem.* **1984**, *88* (2), 181–184.
(54) Inskeep, R. G.; Kelliher, J. M.; McMahon, P. E.; Somers, B. G. *J. Chem. Phys.* **1958**, *28*, 1033–1036.
(55) Tucker, E. E.; Farnham, S. B.; Christian, S. D. *J. Phys. Chem.* **1969**, *73* (11), 3820–3829.
(56) Solomonov, B. N.; Novikov, V. B.; Varfolomeev, M. A.; Klimovitskii, A. E. *J. Phys. Org. Chem.* **2005**, *18* (11), 1132–1137.
(57) Nath, A.; Bender, E. *Fluid Phase Equilib.* **1981**, *7* (3−4), 275–287.

(58) Wolbach, J. P.; Sandler, S. I. *AIChE J.* **1997**, *43* (6), 1597–1604.
(59) Singh, S.; Rao, C. N. R. *J. Phys. Chem.* **1967**, *71* (4), 1074–1078.
(60) Coburn, W. C.; Grunwald, E. *J. Am. Chem. Soc.* **1958**, *80* (6), 1318–1322.
(61) Blainey, P. C.; Reid, P. J. *Spectrochim. Acta Part A: Mol. Biomol. Spectrosc.* **2001**, *57* (14), 2763–2774.
(62) Schwager, F.; Marand, E.; Davis, R. M. *J. Phys. Chem.* **1996**, *100* (50), 19268–19272.
(63) Fletcher, A. N. *J. Phys. Chem.* **1972**, *76* (18), 2562–2571.
(64) Van Ness, H. C.; Van Winkle, J.; Richtol, H. H.; Hollinger, H. B. *J. Phys. Chem.* **1967**, *71* (5), 1483–1494.
(65) Davis, J. C.; Pitzer, K. S.; Rao, C. N. R. *J. Phys. Chem.* **1960**, *64*, 1744–1747.
(66) Fletcher, A. N. *J. Phys. Chem.* **1969**, *73* (7), 2217–2225.
(67) Palombo, F.; Sassi, P.; Paolantoni, M.; Morresi, A.; Cataliotti, R. S. *J. Phys. Chem. B* **2006**, *110* (36), 18017–18025.